NACA RM L53D02

NACA

RESEARCH MEMORANDUM

INVESTIGATION OF A RAM-JET-POWERED HELICOPTER ROTOR ON THE LANGLEY HELICOPTER TEST TOWER

By Paul J. Carpenter and Edward J. Radin

Langley Aeronautical Laboratory
Langley Field, Va.

NATIONAL ADVISORY COMMITTEE
FOR AERONAUTICS

WASHINGTON

June 3, 1953
Declassified December 18, 1953

NATIONAL ADVISORY COMMITTEE FOR AERONAUTICS

RESEARCH MEMORANDUM

INVESTIGATION OF A RAM-JET-POWERED HELICOPTER ROTOR ON THE LANGLEY HELICOPTER TEST TOWER

By Paul J. Carpenter and Edward J. Radin

SUMMARY

A helicopter rotor powered by ram-jet engines located at the rotor blade tips has been tested on the Langley helicopter test tower. The basic hovering characteristics of the rotor and the propulsive characteristics of the ram-jet engine were obtained over a range of corrected tip speeds from 485 to 630 fps and fuel rates from 130 to 310 lb/hr per engine. The rotor was also investigated in the power-off condition and with the engines removed. Additional measurements include the determination of the effects of internal blockage and other modifications on the power-off drag of the jet engines and the determination of the lift and drag of the isolated engines in a small-scale wind tunnel.

The power-on measurements of the propulsive characteristics of the ram-jet engine made on the helicopter tower are compared with the data obtained from free-jet thrust-stand tests in order to evaluate the effects of rotation. A method of analysis for obtaining the net propulsive ram-jet thrust on the free-jet thrust stand and on the tip of a helicopter rotor blade is presented.

INTRODUCTION

Analytical studies have shown that jet-propelled helicopters offer specific advantages over the conventional piston-engine helicopter where high payload for short duration of operation is an important factor. Many of these jet applications consist of units attached to the tip of the rotor blade where, unlike power plants located entirely within the aircraft, they are subjected to aerodynamic and inertia forces at the fastest moving part of the helicopter. The inertia forces increase the structural loads on both the rotor and the engine and also affect the internal flow through the jet engine. The aerodynamic forces directly affect the performance in both normal and power-off flight. In the former condition, both the increased dynamic pressure and the external

drag directly affect the propulsive thrust of the jet engine. In autorotational flight, which would occur following a power failure, the drag of the inoperative jet units may result in excessive descent rates (ref. 1).

Since the over-all performance of a helicopter powered by jet engines mounted on the rotor blade tips is so closely dependent on the aerodynamic and propulsive characteristics of the engine, a study of various jet rotor systems has been undertaken by the National Advisory Committee for Aeronautics to supplement investigations of the separate components of such systems. As the first step in the study of the over-all characteristics of blade-tip jet-propelled rotors, a small ram-jet rotor was investigated on the Langley helicopter test tower. This investigation included the determination of the power-off drag as a function of internal blockage, the power-off lift and drag characteristics of the jet engine as a function of angle of attack, the rotor lift in the power-on condition as a function of fuel flow for various tip speeds, and the engine thrust.

The engine thrust was obtained indirectly from rotor torque measurements. Inasmuch as this calculated engine thrust was much lower than the predicted values, the lift and drag characteristics of the jet engine were studied (power-off condition) in a low-speed wind tunnel and the thrust of the engine was investigated in a small high-speed air jet in order to determine its basic operational characteristics. The method used for reducing the two sets of propulsive thrust data (whirling and nonwhirling conditions) to comparable values is evolved and discussed in the appendix.

SYMBOLS

R	blade radius (measured to inboard side of jet engine), ft
T	rotor thrust, lb
Q	rotor torque, ft-lb
ρ	air density, slugs/cu ft
Ω	rotor angular velocity, radians/sec
C_T	rotor thrust coefficient, $\dfrac{T}{\pi R^2 \rho (\Omega R)^2}$

C_Q rotor torque coefficient, $\frac{Q}{\pi R^2 \rho (\Omega R)^2 R}$

b number of blades

c blade chord, ft

σ rotor solidity, $bc/\pi R$

A_j maximum external cross-section area of jet engine (0.287 ft^2)

D_j total (internal, external, and interference) power-off drag of jet engine

L_j lift of ram-jet engine, lb

V velocity of ram-jet engine, ft/sec

V_c corrected velocity of ram-jet engine, $V/\sqrt{\theta}$, ft/sec

C_{D_j} total (internal, external, and interference) power-off drag coefficient, $\frac{D_j}{\frac{1}{2}\rho V^2 A_j}$

C_{L_j} jet-engine lift coefficient, $\frac{L_j}{\frac{1}{2}\rho V^2 A_j}$

F_p propulsive thrust of jet engine (internal thrust, external drag, and interference drag), lb

W_f mass-flow rate of fuel, lb/hr

S.F.C. specific fuel consumption of ram-jet engine, lb/hr/hp

W_{f_c} corrected fuel mass-flow rate, $W_f/\delta\sqrt{\theta}$, lb/hr

δ ratio of absolute ambient pressure to standard NACA sea-level pressure

θ ratio of absolute static temperature to standard NACA sea-level absolute temperature

$D_{t_{cold}}$ power-off drag of jet engine, $(\text{External drag})_{cold} + (\text{Internal drag})_{cold}$, lb

K support-strut drag plus support-interference drag, lb

K_1 thrust required to accelerate fuel to engine velocity, lb

K_2 mutual interference drag between engine and rotor, lb

APPARATUS

The investigation was made on the Langley helicopter test tower, which is described in reference 2 except for the fuel and ignition system used in these tests. In the power-on tests, the tower drive motor was disconnected from the tower drive shaft so that all the torque required to run the rotor and tower shaft was furnished by the ram-jet engines. A view of the ram-jet-powered rotor mounted on the helicopter tower is shown in figure 1.

Fuel and Ignition System

The fuel (80 octane unleaded gasoline) was pumped through a flow meter at the base of the tower, through tubing above and outside the rotor disk, and then overhead the rotor to a rotating fuel seal located on the axis of rotation. From the rotary seal on the rotor hub the fuel was divided and directed through a 0.045-inch-diameter throttling orifice and flexible tubing to the blades and then through 1/8-inch-inside-diameter steel tubing inside the blades to the jet engines.

Fuel-flow control was difficult to achieve because of the centrifugal pumping action of the blades until the 0.045-inch-diameter metering orifice was installed at the hub on the blade side of the rotating seal. With this orifice installed, the fuel flow was controlled by varying the output pressure (20 to 100 lb/sq in.) of the fuel pump located at the base of the tower. Fuel pressure at the fuel nozzles was supplied mainly by the centrifugal force acting on the column of fuel inside the rotor blades. Ram-jet ignition was obtained by a small spark plug located near the outermost part of the engine shell and partially enclosed to provide a low-air-velocity region for easier ignition at high forward speeds. The high tension spark was provided by a separate coil for each jet unit that was located on the rotor hub.

Rotor Characteristics

The rotor was a two-bladed teetering type with conventional pitch controls and had a radius of 8.72 feet. The blades, which were of all-metal construction, had a constant chord of 8.22 inches and an NACA 0009.5 airfoil section. The radius to the center line of the ram-jet engines was 9 feet. The rotor had the tip engines mounted so that the jet shell was horizontal when the blade pitch angle was 4°, except for the power-off drag against internal blockage tests in which the units were alined with the blade chord. The nature of the blade-jet engine juncture is shown in figure 2. In general, the blade joined the ram-jet shell at approximately a 90° angle with no fillets or smoothly faired curves except at the leading edge. The center of gravity of the jet engine (approximately 7.8 inches from the leading edge of the jet inlet) was located near the quarter-chord station of the airfoil. The static torsional stiffness of the blades was approximately 150 in.-lb/deg of twist.

Ram-Jet Engine

A sketch of the ram-jet engine used is shown in figure 3. This engine had a maximum diameter of 7.25 inches, an inlet diameter of 3.75 inches, an exit diameter of 4.5 inches, a length of 18 inches, and a weight of $9\frac{1}{4}$ pounds. For structural reasons, the ram-jet shell was constructed of Inconel X steel and varied in thickness at the point of attachment to the blade from about 0.25 inch to about 0.05 inch on the outboard side. The flame holder was of the radial finger type with eight equally spaced fingers fastened to the outer shell at the end of the diffuser and pointing forward at a 50° angle to meet at a central point 2.6 inches from the inlet. The fuel nozzles were supported at this junction of the radial fingers. One main nozzle sprayed forward and four smaller nozzles, grouped around the main nozzle, sprayed to the sides and forward at a 20° angle. The forward spraying nozzle was rated at 5.0 gal/hr at a pressure of 100 lb/sq in. The spray pattern was conical, having a dispersion angle of 80°. The inboard, top, and bottom nozzles were rated at 3.5 gal/hr at 100 lb/sq in. with a 60° spray cone angle while the outboard nozzle was rated at 1.5 gal/hr at 100 lb/sq in. with a 60° spray cone angle. This arrangement of side nozzles was used so that more fuel could be sprayed to the inboard side of the jet engine to compensate partially for centrifugal effects on the fuel-spray pattern. For the free-jet thrust-stand tests, the four side nozzles were changed to spray an equal amount of fuel in order to obtain a symmetrical fuel-spray pattern. The forward spraying nozzle for these tests was rated at 15.0 gal/hr at 100 lb/sq in. with a 60° spray cone angle while the four side nozzles were rated at 6.0 gal/hr at 100 lb/sq in.

with an 80° spray cone angle. The nozzle sizes (as mentioned previously) were selected for the free-jet test stand so that a fuel rate comparable to the whirling case could be achieved at the lower fuel pressure available.

METHODS AND ACCURACY

Helicopter Tower Tests

All tests on the helicopter tower were made with ambient wind velocities less than 5 mph and all measurements were obtained under steady-state operating conditions. The test procedure was to hold the rotor tip speed constant by varying the tower or ram-jet-engine power as the rotor thrust was varied through the desired range by varying the blade pitch angle. The methods outlined in reference 2 were used to establish thrust and torque tares for both the power-off and power-on operating conditions.

The performance of the rotor with and without the "cold" (power-off) jet engines attached was determined directly from the conventional tower drive-shaft measurements of thrust and torque. The effects of the cold jet engines on rotor thrust were studied by comparing the measured rotor thrust coefficients for the two conditions at fixed blade-root angles of attack. This approach neglects possible effects of blade twist introduced by addition of the engines; however, such effects would be expected to be small because of the high torsional stiffnesses of the test blades. The cold drag of the jet engines was determined in a similar manner from the differences in rotor torque coefficient obtained at 0° blade angle for the rotor alone and for the rotor with the engines installed at 0° incidence. The cold drag of the engines so defined includes a small increment corresponding to the total interference drag between the rotor and the tip engines. This increment interference drag would be expected to be somewhat different from the interference drags occurring in other operating conditions because of the effects of engine incidence, blade angle of attack, and engine thrust.

The cold drag of the engines was determined both with the original fuel nozzles and flameholders installed and with various amounts of internal blockage ranging from zero (nozzles and flameholders removed) to the completely closed condition. The internal blockage was varied by inserting plugs in a perforated disc mounted at the end of the diffuser. The percent blockage was defined as the ratio of the actual blocked area to the maximum internal area.

In the power-on-engine operating condition, the rotor thrust again was determined directly from the tower-shaft thrust measurements. The tower-shaft torque measurements, however, did not give either the engine

thrust or the rotor torque which it counterbalanced. The propulsive thrust of the engine, therefore, was calculated indirectly by the method outlined in the appendix. This method assumed, in essence, that the torque overcome by the jet engines was equal to the torque of the basic rotor without tip engines at the same rotor thrust coefficient plus the torque chargeable to fuel pumping within the blades plus an increment in torque corresponding to the mutual interference drag between the rotor and the tip engines.

The estimated accuracies of the basic quantities measured in the tower tests are as follows: rotor thrust, ±15 pounds; rotor torque, ±10 foot-pounds; blade pitch angle, ±0.1°; fuel-flow rate, ±10 lb/hr; and rotor angular speed, ±1 rpm. The over-all accuracy of the plotted results is believed to be ±3 percent.

Wind-Tunnel Tests

Rough measurements of the lift and total drag characteristics of the isolated cold-jet engine were obtained in the 1/15-scale model (2- by 4-foot test section) of the Langley full-scale tunnel at an airspeed of about 140 fps. The model was mounted for the tests on a 1/2-inch-diameter rod which was rotated to change the angle of attack. Forces were measured by a strain-gage balance located outside the jet. The drag measurements were corrected for longitudinal bouyancy and for the strut and fitting tare determined by additional tests with an image support system. When the sensitivity of the balance is taken into account, it is estimated that the over-all accuracy of these wind-tunnel data is about ±5 percent in drag coefficient and ±3 percent in lift coefficient. It should be noted that the Reynolds number based on body length was only about 1×10^6 for these tests compared with about 3.5×10^6 for the tower tests.

Free-Jet Thrust-Stand Tests

The thrust and fuel consumption of the ram-jet engine were also determined on a free-jet thrust stand (a small high-speed air jet) in order to obtain a comparison of the static thrust of the engine with the thrust values calculated for the whirling condition. The free-jet was 7.6 inches in diameter and had a maximum corrected air speed of 647 fps. The jet engine was strut-mounted at 0° angle of attack in the air jet approximately 14 inches from the free-jet nozzle. This distance was chosen since it was the closest location at which the jet engine did not raise the static pressure in the free-jet nozzle. As in the case of the wind-tunnel tests, a strain-gage balance at the base of the support strut was used to measure the net force. Force measurements were obtained without combustion as well as for the complete range of fuel flows within which combustion could be maintained.

The method of determining the ram-jet propulsive thrust from the free-jet thrust-stand measurements is discussed in the appendix. Briefly, the method consists of adding the measured power-on (thrust minus external drag plus support drag) value to the measured power-off total-drag value and subtracting from the sum the value of the power-off total drag of the ram jet immersed in an infinitely large airstream as determined in the power-off whirling tests. In order to eliminate any influence of the estimate of the power-off total drag on the comparison of the engine thrusts in the whirling and free-jet test condition, these thrusts are compared on the basis of the parameter

$$(\text{Thrust} - \text{External drag})_{\text{power on}} + (\text{Total drag})_{\text{power off}}$$

which can be shown to be valid, as well as on the basis of the estimated propulsive thrust

$$(\text{Thrust} - \text{External drag})_{\text{power on}}$$

The free-jet thrust and drag measurements are believed to be accurate to ± 0.25 pounds and the over-all accuracy of the plotted results is believed to be approximately equal to that for the tower tests.

RESULTS AND DISCUSSION

Power-Off Aerodynamic Characteristics of Ram-Jet Engine

The power-off total drag coefficients of the ram-jet engines determined in the tower tests for the conditions of 0° angle of attack and 0° engine incidence are presented in figure 4 as a function of the internal area blockage. The results indicate that the engine drag remained essentially constant until the internal area was blocked over 80 percent. The curve also shows that the drag coefficient was reduced from 0.145 to about 0.087 by completely blocking off the internal flow. In order to determine the effectiveness of an exit fairing in further reducing the cold drag, a tail cone fairing about 6 inches long was fastened to the jet engine. The drag decrement due to the tail cone (which also provides 100 percent blockage) decreased the drag coefficient to 0.073. Since most of this reduction can be achieved by blocking off the flow, which has been successfully employed in at least one practical application, the additional complications required for providing a tail cone fairing do not appear to be justified.

The leading-edge radius of the original engine was increased in one phase of the tests from 0.1 inch to 0.3 inch to determine if such a modification would reduce the internal drag at the higher mass flows for which internal-flow separation was suspected. This modification reduced the total drag by about 10 percent for the condition of zero internal blockage for which the inlet mass flow was highest, but did not have any effect when the internal blockage was 30 percent or more with correspondingly lower inlet mass flows. The change in leading-edge radius did not appear to affect the external flow inasmuch as the drag coefficients for both configurations were the same for blockages of 30 percent or greater.

The power-off drag coefficient of the isolated ram jet as determined by the small-scale wind-tunnel tests made with the normal flameholders and nozzles installed is also shown in figure 4. The difference between the ram-jet drag obtained from the rotor tests and that from wind-tunnel tests indicates the existence of an interference drag in the case of the data obtained from the tower tests. The magnitude of the indicated interference is not reliable, however, because of accuracy limitations and because of differences in Reynolds number.

The lift and drag characteristics obtained in the small-scale wind-tunnel tests of the isolated ram-jet engines are shown as a function of angle of attack in figure 5 for the configuration with the normal flameholders and nozzles. In order to obtain an estimate of the drag-coefficient variation with angle of attack for the unit attached to the rotor blade tip, a modified drag-coefficient polar was established by adding to the drag polar obtained in the wind tunnel an increment equal to the difference between the wind-tunnel tests and the rotor tests at 0° angle of attack. This polar will be used in a subsequent analysis of rotor-engine interference effects. The cold drag of the unit is about 75 percent greater at 11° angle of attack than at 0°. This large increment in cold drag would adversely affect the autorotative characteristics of the rotor. A study of the external and internal flow over and through the jet engine (engine at 0° angle of attack) was made in the 1/15-scale model of the full-scale wind tunnel. The air flow over the external surface of the engine was unseparated, whereas the internal flow became separated a short distance behind the diffuser inlet station. Some decrease in over-all drag might be accomplished by delaying the separation of the internal flow. Mounting the ram-jet engine in bearings so that it is free to remain at 0° angle of attack, regardless of the blade pitch setting, therefore, may be advantageous. A possibility for decreasing the external drag of the jet engine is that of redesigning the ram-jet engine so that it can be partially submerged in the blade structure to extend effectively the blade lifting surface.

The lift data presented in figure 5 indicate that the slope of the lift curve for this engine is constant for the range of angle of attack presented and has a value of about 0.04 per degree.

The effect of the tip-mounted jet engine (power-off condition) on the rotor thrust coefficient obtained over a range of blade-root pitch angles at a tip speed of 530 fps is shown in figure 6. Since the blade pitch is measured at the root, the plot does not show how much of the increased rotor thrust coefficient is due to the lift of the ram-jet engine because of possible blade twist caused by pitching moments on the jet engine and of the end-plate effect of the jet engine on the rotor blade. The possible significance of these effects is illustrated by the fact that the increment in thrust coefficient indicated for a blade-root pitch setting of 8° would be obtained as a result of the blade twisting only a quarter of a degree.

The lift of the tip-mounted ram jet for various blade angles was calculated from the relationship of lift coefficient and angle of attack presented in figure 5. This lift was then plotted in figure 6 as equivalent rotor thrust coefficient against blade-root pitch angle. It is seen that the increment in rotor thrust with and without the engines is approximately equal to the increment calculated from the wind-tunnel lift-coefficient data of the isolated jet engine. This result indicates that the end-plate effect of the tip engine is either negligible or is completely compensated for by a negative pitching moment introduced by the engine that washes out the blade tip.

The calibration of the rotor for the blades alone and for the blades with ram-jet engines attached at an angle of incidence of -4° (power-off) is presented in figure 7 as curves of rotor thrust coefficient against rotor torque coefficient. A dashed-line curve is also presented in figure 7 which represents the addition of the calculated equivalent rotor torque and thrust coefficient of the ram-jet engines (calculated from the wind-tunnel lift and adjusted drag polar shown in fig. 5) to the blades alone curve. A blade twist of as much as 1° or 2° would be expected to have a negligible effect on the location of the experimental curve for the rotor with engines attached. The general agreement of this curve with the dashed-line curve, therefore, demonstrates that the net interference effects were very small except at the higher rotor thrust coefficients. It appears probable that the aerodynamic effects of adding a ram-jet engine to the tip of a rotor can be estimated from wind-tunnel results for the isolated engine with reasonable accuracy in most cases, unless the pitching-moment characteristics of the engine and the torsional stiffness characteristics of the blade are such as to cause a large amount of blade twisting.

Propulsive Characteristics of the Ram-Jet Engine

The variation of ram-jet thrust plus total power-off engine drag obtained in the tower tests is shown in figure 8 as a function of fuel flow for various rotor speeds. The data have been corrected to standard sea-level conditions by the method outlined in reference 3 from the ambient pressure and the ambient temperature plus an average temperature rise of 50° F in the plane of the ram jets. This temperature rise of 50° F, which was determined by a thermocouple 2 inches ahead of the inlet and fluctuated ±10° over a range of blade pitch angle from 0° to 5°, is the increment by which the measured temperature rise exceeded the calculated adiabatic temperature rise because of flow contamination by the preceding engine. The temperature rise is applicable only to the present configuration in the flight condition of hovering out of ground effect and was introduced only to make the results directly comparable to the free-jet test-stand results. The corrected ram-jet velocities $V/\sqrt{\theta}$ are 630, 576, 529, and 485 fps. The uncorrected velocities were 668, 617, 555, and 515 fps, respectively. The range of blade-root pitch angle for the power-on data was from 0° at the lowest thrust point to approximately 5° at the maximum points resulting in ram-jet angles of attack from approximately -4° to 1°. A curve of propulsive thrust plus power-off drag obtained on the free-jet thrust stand at a corrected air velocity of 613 fps is also shown. The method of obtaining these thrust and drag values is discussed in the appendix.

As indicated in the appendix, a comparison of the two curves is believed to afford a valid indication of the effects of whirling on engine performance. The flattening of the two top curves indicates that a stoichiometric fuel-air mixture may have been attained prior to the rich blowout. The cross over of the whirling and free-jet test-stand curves at the lower fuel rates may have been due to local regions having a fuel-air ratio high enough to burn more efficiently. The difference in maximum thrust between the free-jet test stand and whirling tests (at velocities of 613 and 630 fps, respectively) is attributed mainly to distortion of the fuel-spray pattern due to centrifugal effects. The results given in figure 8 are replotted in figure 9 in terms of the estimated propulsive thrust against fuel-flow rate. The same conclusions can be drawn from figure 9 as from figure 8. At a corrected velocity of 613 fps, the maximum propulsive thrust for the whirling case is indicated to be approximately 21 percent less than that measured for the free-jet thrust stand.

A convenient method of evaluating engine performance is in terms of specific fuel consumption in lb/hr/hp for various air velocities as shown in figure 10 for both the whirling and free-jet test-stand results. The lowest specific fuel consumption of 12.1 lb/hr/hp for the whirling case and about 9.4 lb/hr/hp on the free-jet thrust stand occurred at the highest speed for both cases. The results indicate that, at a

corrected velocity of 630 fps, the specific fuel consumption is about 29 percent greater as compared to free-jet thrust-stand operation. This difference is again attributed, of course, to the effects of centrifugal distortion of the fuel-spray pattern.

Effects of Fuel Distribution on Engine Performance

Various arrangements of fuel nozzles were tried for the helicopter tower tests including equally rated nozzles to give a symmetrical spray pattern similar to that for the free-jet tests. Of the fuel nozzle arrangements tested, the ram-jet engine would operate satisfactorily in the whirling condition only with the arrangement described in the section on "Apparatus."

Free-jet test-stand results showed that the engine thrust is very sensitive to fuel spray wetting the walls. For example, on the free-jet test stand, when larger fuel nozzles were used, some of the fuel droplets impinged on the engine wall. A large reduction of engine thrust resulted with the magnitude of the reduction depending on the relative amount of fuel wetting the walls. This result indicates that the whirling performance also would be decreased if fuel particles were thrown against the outer wall of the engine under the influence of high centrifugal forces, particularly at the high tip speeds (668 fps uncorrected) at which centrifugal loads are of the order of 1500g.

Fuel stains observed inside the burner after a typical whirling test run indicated that a considerable amount of fuel actually was being thrown against the outboard wall of the engine. The fuel stains were in the form of an irregular teardrop shape with the blunt end forward. Various shades of discoloration were present within the boundaries of the wetted area. The stains probably were due to the difference in temperature of the ram-jet shell brought about by the cooling effect of the collected fuel. A small hole was drilled through the engine shell on the outboard side of the engine, where evidence of fuel collection was noted, to allow for the drainage of the excess fuel. This procedure appeared desirable, because under the high centrifugal loading at the higher tip speeds, a small difference between jet engines in the amount of collected fuel could produce a considerable unbalanced force on the rotor.

Some calculations have been made (ref. 4) of the paths of various sized fuel particles issuing from a forward-pointing nozzle alined with the airstream and subjected to large centrifugal accelerations. For those conditions, representative of the ram-jet rotor tested, the results indicate that a significantly large number of particles (0.002 inch or larger in diameter) would impinge on the wall of the diffuser and combustion chamber. There is little or no information available on the

particle spectrum characteristics of the fuel-spray nozzles used, although literature on fuel nozzle sprays indicate that it is reasonable to assume that fuel particles 0.002 inch and greater in diameter would be present. This general problem of centrifugal effects will be present to some extent (but not necessarily as serious) on all helicopter jet systems in which liquid fuel is burned at the blade tip.

Contamination by Preceding Engine

The possibility of the decreased whirling thrust being caused by contamination effects, in which the exhaust of one engine contaminates the intake air of the other engine, was also considered. Flow studies of the air at the blade tips with the rotor hovering out of ground effect were made by locating a smoke source in the ram-jet engine. The results indicate that, at the normal blade pitch setting of 4°, there is an upward flow of the exhaust gases in the plane of the ram jets. The exhaust leaves the jet engine, moves upward out of the ram-jet path, moves radially inboard, and is sucked through the rotor disk. The individual smoke filaments issuing from the jet-engine exhaust show that the following ram-jet engine misses the exhaust of the preceding engine for blade pitch settings greater than 3°. Despite smoke studies indicating offset of the exhaust where the engine missed the exhaust of the preceding engine, there was a temperature rise of 50° over and above the adiabatic value. This 50° F temperature rise caused a loss of approximately 5 percent in maximum thrust. This loss, although important, is small compared with the losses caused by centrifugal effects. It should be remembered also that this loss would be decreased or eliminated entirely in the forward flight conditions where the engines do not track.

Rough Operation and Blowout

Another problem associated with the ram-jet engine consists of rough operation and blowout. Under whirling conditions at a corrected velocity of 630 fps, this engine experienced lean blowout at a fuel flow of about 195 lb/hr. Rich blowout occurred at a fuel rate of about 310 lb/hr following rough and erratic operation which began at a fuel rate of about 270 lb/hr. On the free-jet thrust stand at the corrected airspeed of 613 fps, the value for lean blowout was about the same; however, neither rough, erratic operation nor rich blowout was encountered up to fuel rates of 400 lb/hr. Therefore, it appears that the problem of rough operation and rich blowout is also aggravated by the centrifugal effects on the fuel-spray pattern.

Possibilities for Improving Engine Performance

The results of these tests indicate that an appreciably wider range of stable operation and gains in combustion efficiency which will result in significant gains in both thrust and specific fuel consumption will be realized by decreasing the sensitivity of the ram-jet engine to fuel-spray distortion caused by the centrifugal acceleration at the rotor tip. One possibility for improving the fuel distribution may be that of skewing the combustion chamber along the line of the fuel-particle paths to prevent these particles from impinging on the combustion chamber wall. Another possibility may be the use of more atomizing nozzles or of vaporizing the fuel by preheating in order to reduce the size and weight of the individual fuel particles. The gain in maximum thrust possible through the mechanism of an increase in combustion efficiency may be particularly significant, inasmuch as the leveling off of the thrust against fuel-rate curves of figures 8 and 9 for a corrected velocity of 630 fps indicates that little, if any, further gain in combustion temperature can be attained by merely increasing the fuel rate even if blowout could be avoided. The possibility that the maximum thrust can be further increased by modifications to reduce the burner drag also should be considered. This type of development work was considered to be beyond the scope of this investigation.

Power-on Rotor Characteristics

The hovering performance of the ram-jet rotor is presented in figure 11 in terms of the variation of corrected rotor thrust with corrected total (2 ram jets) fuel consumption for rotor tip speeds from 500 to 648 fps. The maximum rotor thrust was obtained at the highest speed. Where maximum rotor thrust is not needed, however, higher ratios of rotor thrust per pound of fuel may be obtained at lower tip speeds. For example, if a rotor thrust of only 400 pounds is needed, such as may be the condition near the end of a flight, the fuel rate could be reduced from about 465 to about 440 lb/hr by reducing the tip speed from 648 to 539 fps. This apparent paradox (for the ram-jet engine) of increased performance at lower tip speeds is caused by operation at more nearly optimum rotor lift-drag ratios and increased ram-jet burning efficiency due to reduced centrifugal fuel-spray distortion. These factors more than compensate for the reduction of ram velocity.

From the foregoing discussion and from references 1 and 5 it is apparent that the matching of the rotor to the engine is a consideration of major importance. If the rotor solidity is selected for optimum performance in the autorotative condition, the maximum possible rotor thrust in power-on flight is decreased and, at a rotor thrust less than the maximum, increased over-all (rotor and engine) efficiency can be achieved by operating at tip speeds less than the maximum. On the other hand, selection of the rotor solidity for the maximum-thrust operating condition may

lead to unacceptable performance in the autorotative (power-off) condition. For the power-on case, at a blade tip speed of 650 fps, the blade loading parameter C_T/σ for a rotor thrust of 600 pounds is about 0.05. Normally, for an efficient rotor, the value of C_T/σ should be about 0.1. In the event of a power failure, however, the tip speed would be reduced to about 400 fps to reduce the power losses incurred by the inoperative ram-jet engine, thus reducing the rate of descent. This result increases the value of C_T/σ of the rotor from 0.05 to about 0.13 which is about the maximum that can be obtained without blade stall. From these considerations, it can be seen that efficiency in power-on flight was sacrificed for more satisfactory performance in case of a power failure for the present investigation.

CONCLUSIONS

The basic hovering characteristics of a typical ram-jet-powered helicopter rotor and the aerodynamic and propulsive characteristics of the ram-jet engine have been determined on the Langley helicopter tower. The aerodynamic and thrust characteristics of the isolated engine have also been studied in small free-jets. The more pertinent findings of this preliminary investigation are as follows:

1. The power-off drag coefficient of the engine was essentially constant up to an internal blockage of 80 percent. The drag coefficient was reduced from 0.145 to about 0.087 by completely blocking off the internal flow. A further reduction to 0.073 was obtained by using a tail cone fairing.

2. The power-off total drag of the jet engine which is important for autorotative operation was approximately 75 percent greater at 11° angle of attack than at 0°. This large increment indicates that mounting the ram-jet engine on bearings so that the angle of attack of the engine remains near zero may be advantageous.

3. The specific fuel consumption of the ram-jet engine, when whirling at a tip speed of 630 fps with a centrifugal loading of about 1500g, was about 29 percent greater than that obtained on a free-jet thrust stand. Similarly, the maximum engine propulsive thrust developed for the whirling case was approximately 21 percent less than that measured on the free-jet thrust stand. This phenomena is attributed mainly to distortion of the fuel-spray pattern under high centrifugal loadings and is a general problem for all tip-located jet power plants involving burning at the blade tips.

4. Although there exists some effect of contamination on the jet engine thrust, as indicated by smoke-flow observations, and the measured 50° F temperature rise at the inlet, the over-all effect on thrust is small compared with the more adverse centrifugal effects.

5. The interference effects between the engine and rotor were indicated to be small within the range of the test conditions.

6. The matching of the rotor to the engine involves important design compromises between a rotor designed for efficient power-on operation and a rotor designed for acceptable autorotative characteristics.

Langley Aeronautical Laboratory,
National Advisory Committee for Aeronautics,
Langley Field, Va.

APPENDIX

The problem of determining the performance of the ram-jet engine mounted on the rotor tips is complicated by the lack of a direct means for measuring the engine thrust and by mutual interference effects between the rotor and the engines. The determination of the performance of a stationary engine in a large wind tunnel generally is much simpler. In a small air jet (free-jet) such as that used in the present case, however, the problem again becomes complicated inasmuch as the measured external drag generally is lower than the value that would be measured in an infinitely large airstream, such as is encountered at the tip of the rotor blade. Thus, any comparison between propulsive thrust and specific fuel-consumption data obtained in the whirling condition and on the usual type of ground test stand must be made with care. A method of comparing the whirling and the free-jet thrust-stand propulsive characteristics of a ram-jet engine which takes into consideration the major effects of the aforementioned complications has been evolved and is presented herein (fig. 12).

Analysis of Data From Free-Jet Thrust Stand

For the free-jet thrust stand, let $F_p - K$ be the force measured during combustion and $D_{t_{cold}} + K$ the force measured without combustion. The directions are indicated in the following sketch:

Then

$$F_p - K = \text{Internal thrust} - (\text{External drag})_{hot} -$$

$$\text{Mounting strut drag} - \text{Support interference drag}$$

and

$$D_{t_{cold}} + K = (\text{External drag})_{cold} + (\text{Internal drag})_{cold} +$$

$$\text{Mounting strut drag} + \text{Support interference drag}$$

By the addition of the two equations, $F_p + D_{t_{cold}}$ is obtained and the mounting strut-drag and support interference-drag terms drop out of the expression. This term $F_p + D_{t_{cold}}$ can be determined accurately on the free-jet thrust stand. The separation of this quantity into its two components in order to obtain the propulsive thrust as conventionally defined requires that the true cold drag be known. In the present investigation this separation was obtained from cold-drag rotor tests of the ram jet in which the blade pitch and ram-jet angle of attack was 0°.

It is recognized that this cold drag includes some unknown increment of interference drag between the tip-mounted jet engine and the rotor blade; however, this increment should be very small when the blade and ram jet are each set at 0° angle of attack.

Analysis of Data From Whirl Tests

In order to determine the thrust output of the ram-jet engine mounted on the helicopter rotor blade, it was first necessary to determine the thrust and torque characteristics of the rotor without the jet engines attached. After these characteristics were determined the jet engines were attached to the blades and the rotor was tested over the range of thrust coefficients and tip speeds with the ram jets supplying all the required torque. From the previous tests of the blades alone, the rotor torque required to produce a given rotor thrust at a given tip speed was known. It also was known that the tower-shaft tare was negligible. The rotor torque value was divided by the number of ram jets and the ram-jet center line radius to obtain the part of the propulsive thrust of the jet engine used to overcome the torque of the blades themselves. Inasmuch as the thrust-torque polar for a rotor is relatively insensitive to a small amount of blade twist, any twist of the blade that might be introduced by pitching moments of the engine would be expected to have a negligible effect on the correctness of the value.

A second component of the engine thrust which must be added in accounting for the total thrust furnished by the engine is that required to accelerate the fuel from zero velocity at the rotor hub to the speed of the jet engine. This force to accelerate the fuel mass is simply mV_j where m is the mass flow of fuel per second and V_j is the jet-engine velocity. No further correction was made to account for the forward spraying of part of the fuel since the momentum of the forward fuel-spray mass was negligibly small. It was also negligible in the free-jet stand tests and, consequently, was not applied to these results either.

In addition to the two items of thrust just discussed, the engine must supply also the thrust necessary to overcome the mutual interference drag of the engine-rotor combination. The interference drag could not

be determined directly, but the sum of the total cold drag plus the interference drag could be obtained. The first step was to calibrate the rotor with the jet engines attached in the normal configuration (-4° incidence to blade chord line) and inoperative in order to determine the variation of torque and thrust coefficients for the rotor blades and ram-jet combination. The sum of the jet engine cold drag and mutual interference drag at a given thrust coefficient was represented by the difference in torque coefficient between the curves representing the blades alone and blades with ram-jet engines attached. This difference in torque coefficient was converted to ram-jet cold drag plus interference drag for each ram-jet power-on condition.

When the ram jets were operated there was a temperature rise of approximately 50° F in the core of air traversed by the engine because of heating by the preceding engine. This heating decreased the density of the air in the immediate vicinity of the ram jet and resulted in lower effective drag and interference losses. Therefore, the sum of the cold drag and interference drag calculated from the difference between the torque coefficients at a constant thrust coefficient was decreased by a factor representing the ratio of density of the heated air to the ambient air.

Comparison of Results

A comparison of the values of $F_p + D_{t_{cold}}$ obtained by the two methods is considered to be valid and is presented in figure 8. Inasmuch as this is not a familiar quantity, however, a total engine cold drag corresponding to the drag coefficient of 0.145 determined from the whirl tests at 0° blade angle and engine incidence (and which is considered to be essentially free of interference effects) was subtracted from each of the $F_p + D_{t_{cold}}$ values in order to obtain a qualitative indication of the effects of whirling in terms of the net propulsive thrust of the engine F_p or the corresponding S.F.C. These results are given in figures 9 and 10.

The engine performance parameters have been corrected in accordance with reference 3.

REFERENCES

1. Gessow, Alfred: An Analysis of the Autorotative Performance of a Helicopter Powered by Rotor-Tip Jet Units. NACA TN 2154, 1950.

2. Carpenter, Paul J.: Effect of Wind Velocity on Performance of Helicopter Rotors as Investigated With the Langley Helicopter Apparatus. NACA TN 1698, 1948.

3. Sanders, Newell D.: Performance Parameters for Jet-Propulsion Engines. NACA TN 1106, 1946.

4. Katzoff, Samuel, and Smith, Samuel L., III: A Theoretical Analysis of the Distortion of Fuel-Spray-Particle Paths in a Helicopter Ram-Jet Engine Due to Centrifugal Effects. NACA RM L53A02, 1953.

5. Gustafson, F. B., and Gessow, Alfred: Effect of Rotor-Tip Speed on Helicopter Hovering Performance and Maximum Forward Speed. NACA WR L-97, 1946. (Formerly NACA ARR L6A16.)

Figure 1.- View of ram-jet-powered helicopter rotor mounted on test tower.

Figure 2.- Ram-jet engine-blade combination used for whirling tests on helicopter test tower.

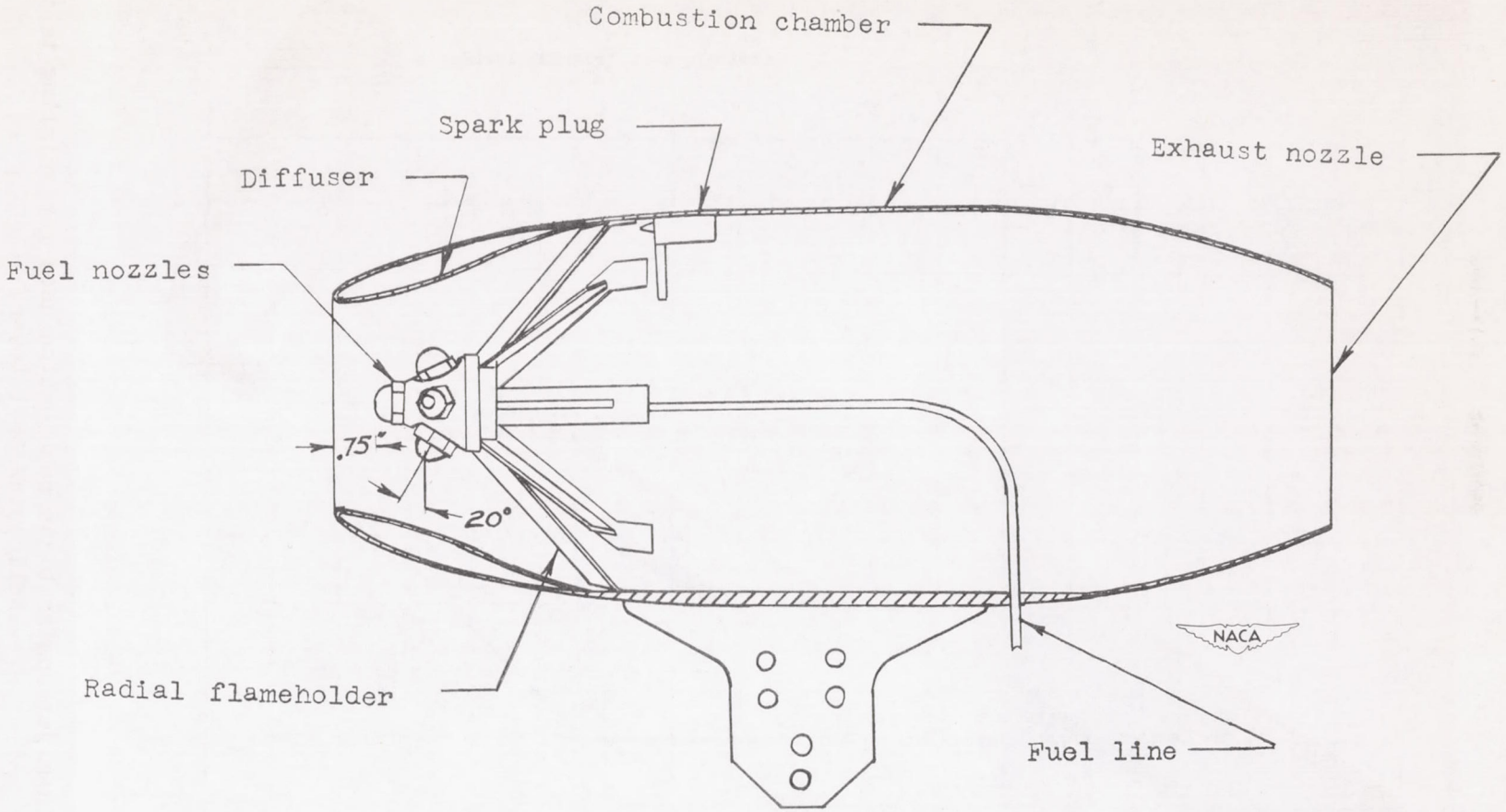

Figure 3.- Sketch of ram-jet engine. Jet shell and flameholder are made of Inconel X steel.

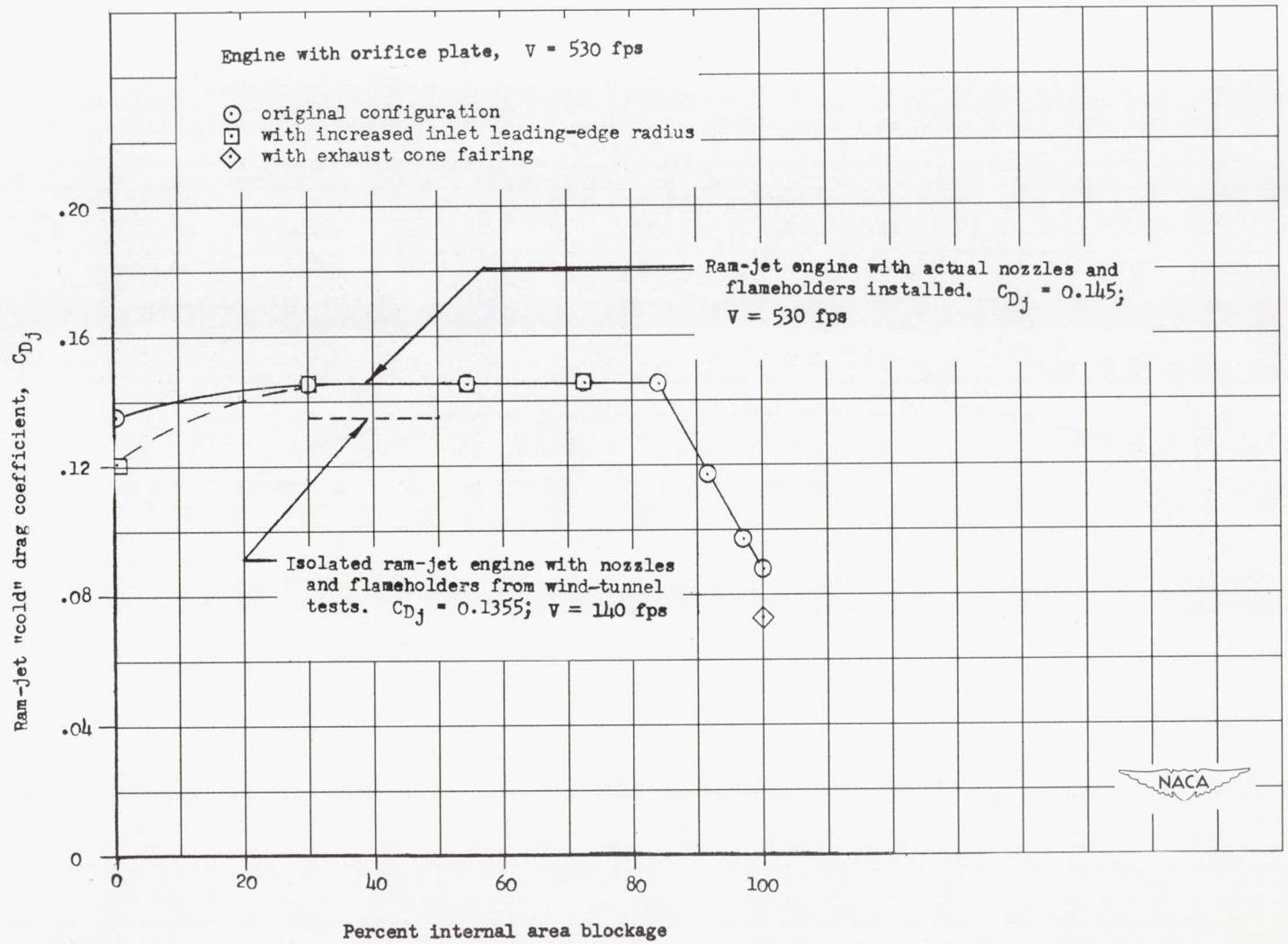

Figure 4.- Power-off drag coefficient as a function of internal blockage at 0° angle of attack and 0° engine incidence.

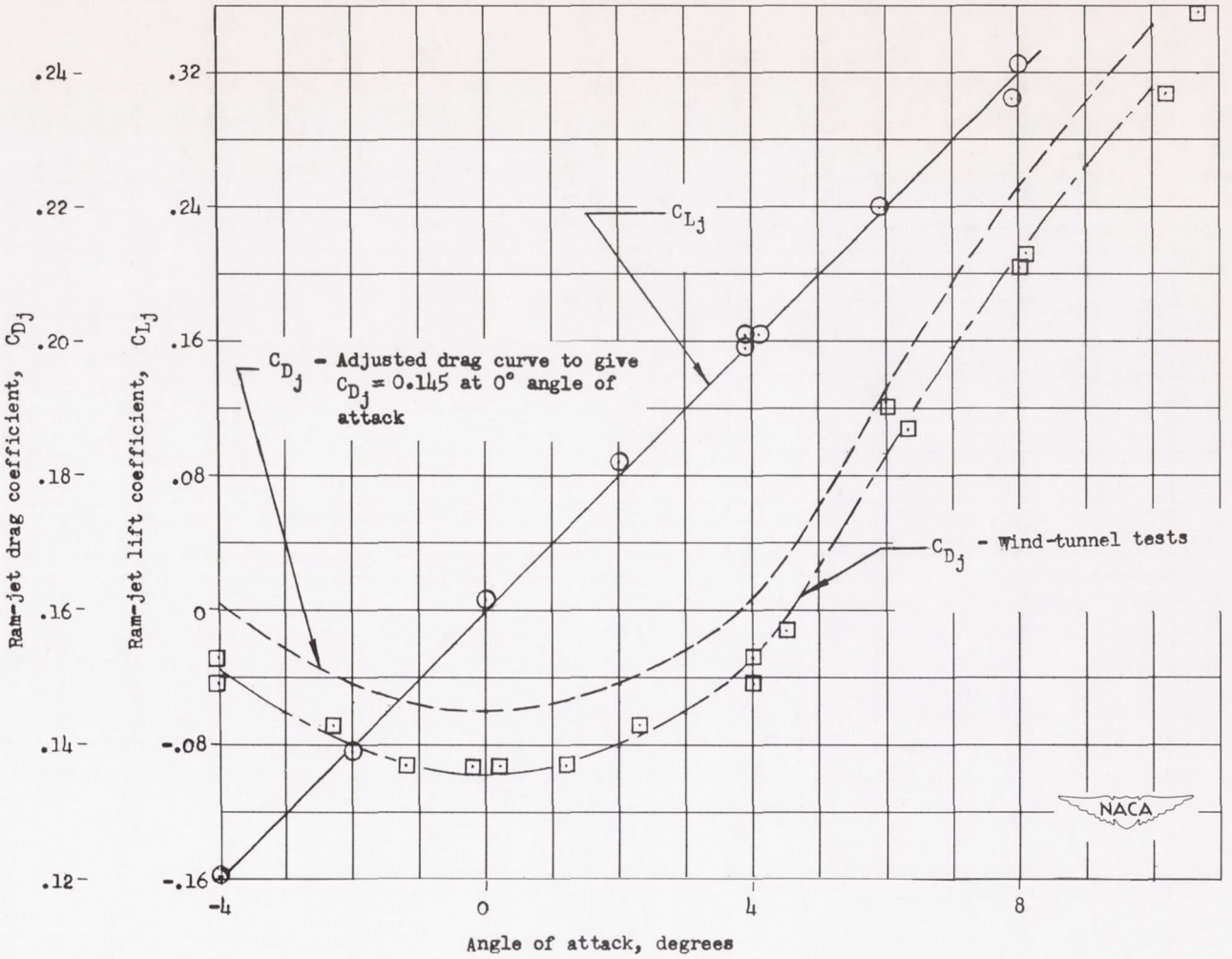

Figure 5.- Lift and drag characteristics of ram-jet engine for various angles of attack determined by wind-tunnel tests at a velocity of approximately 140 fps.

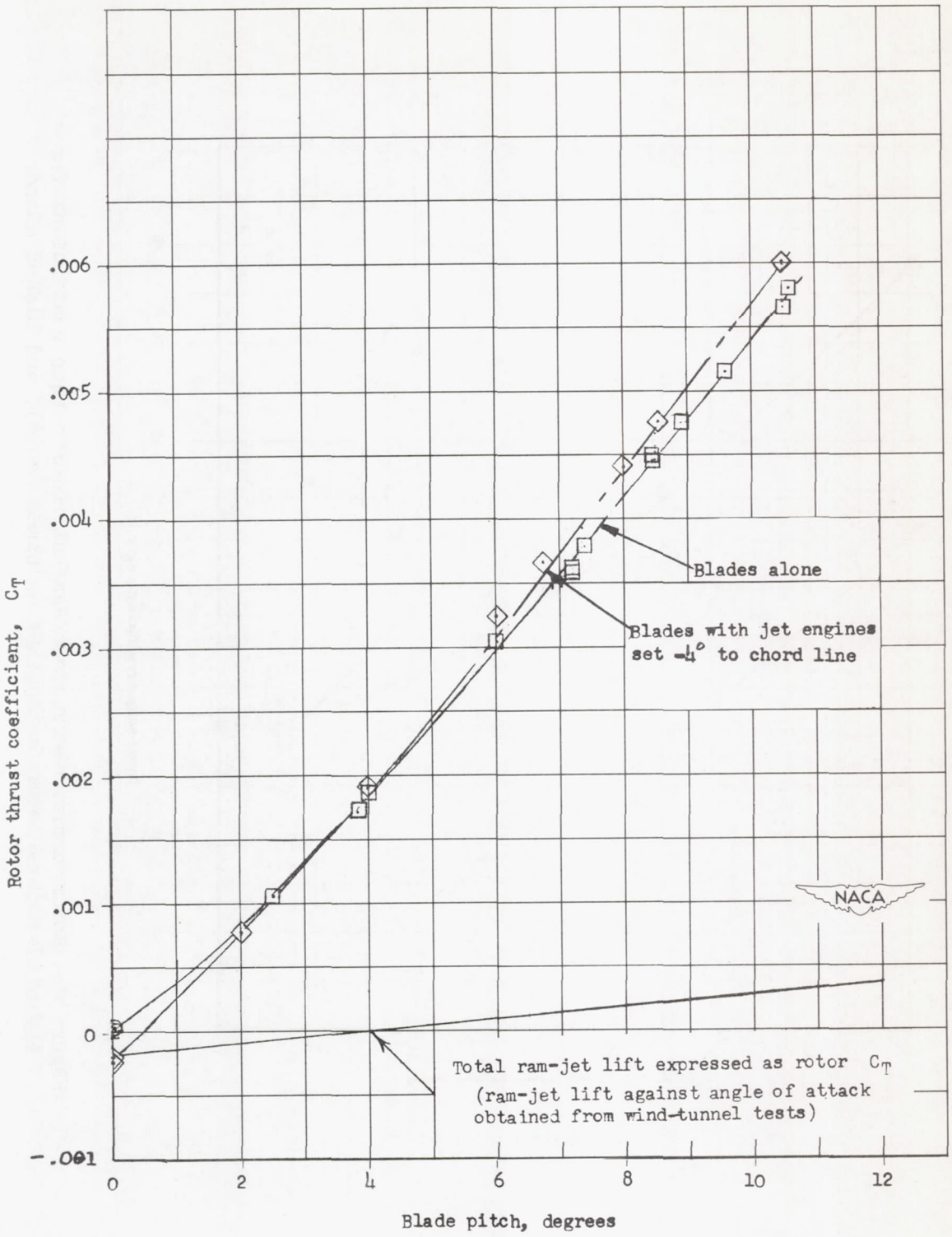

Figure 6.- Effect of ram-jet engine on rotor thrust coefficient for various blade pitch settings. Power off; rotor ram-jet speed, 530 fps.

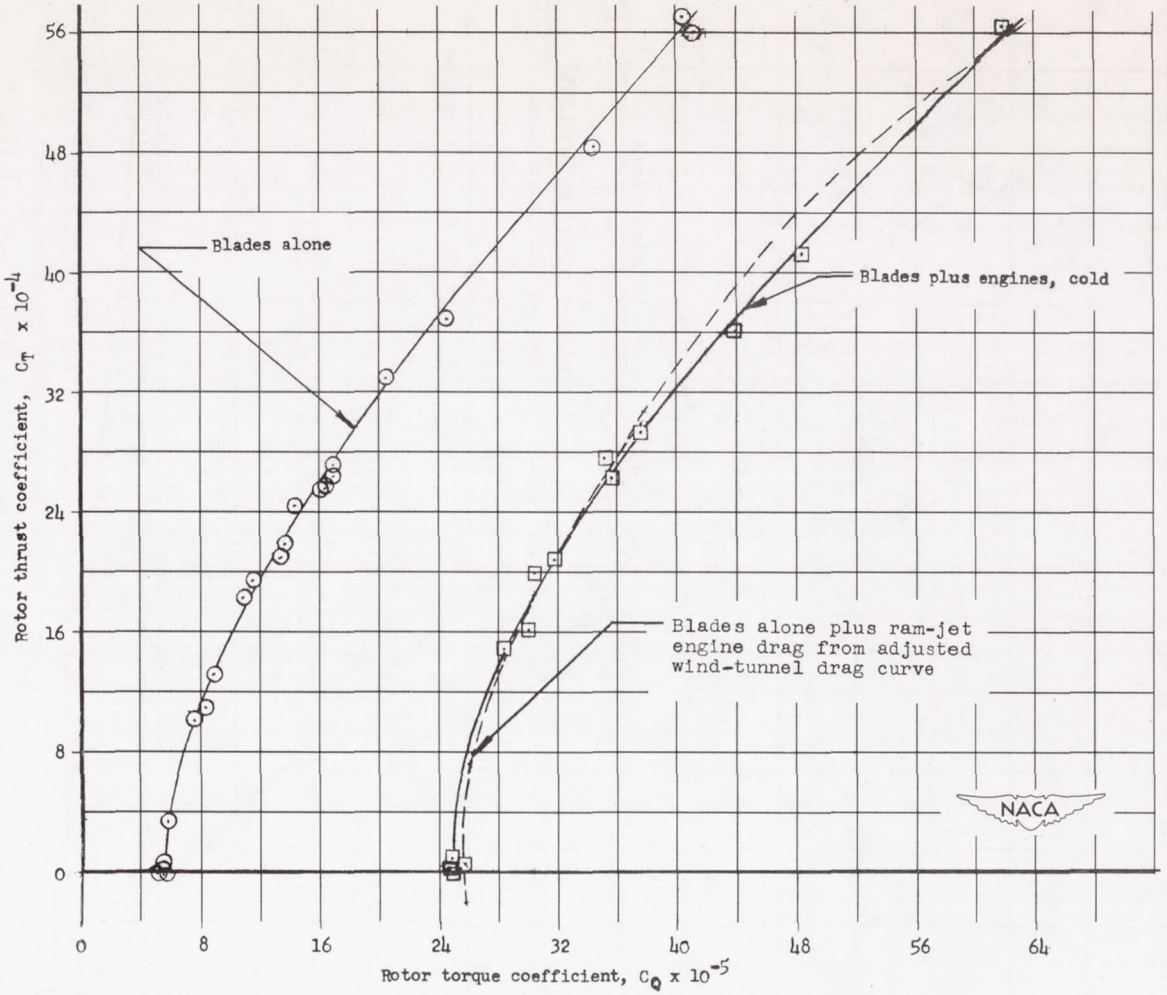

Figure 7.- Rotor thrust coefficient against rotor torque coefficient for the blades alone, ram-jet engines on blade (cold), and blades alone plus ram-jet engine drag from adjusted wind-tunnel drag curve. Tip speed, 530 fps; tunnel velocity, 140 fps.

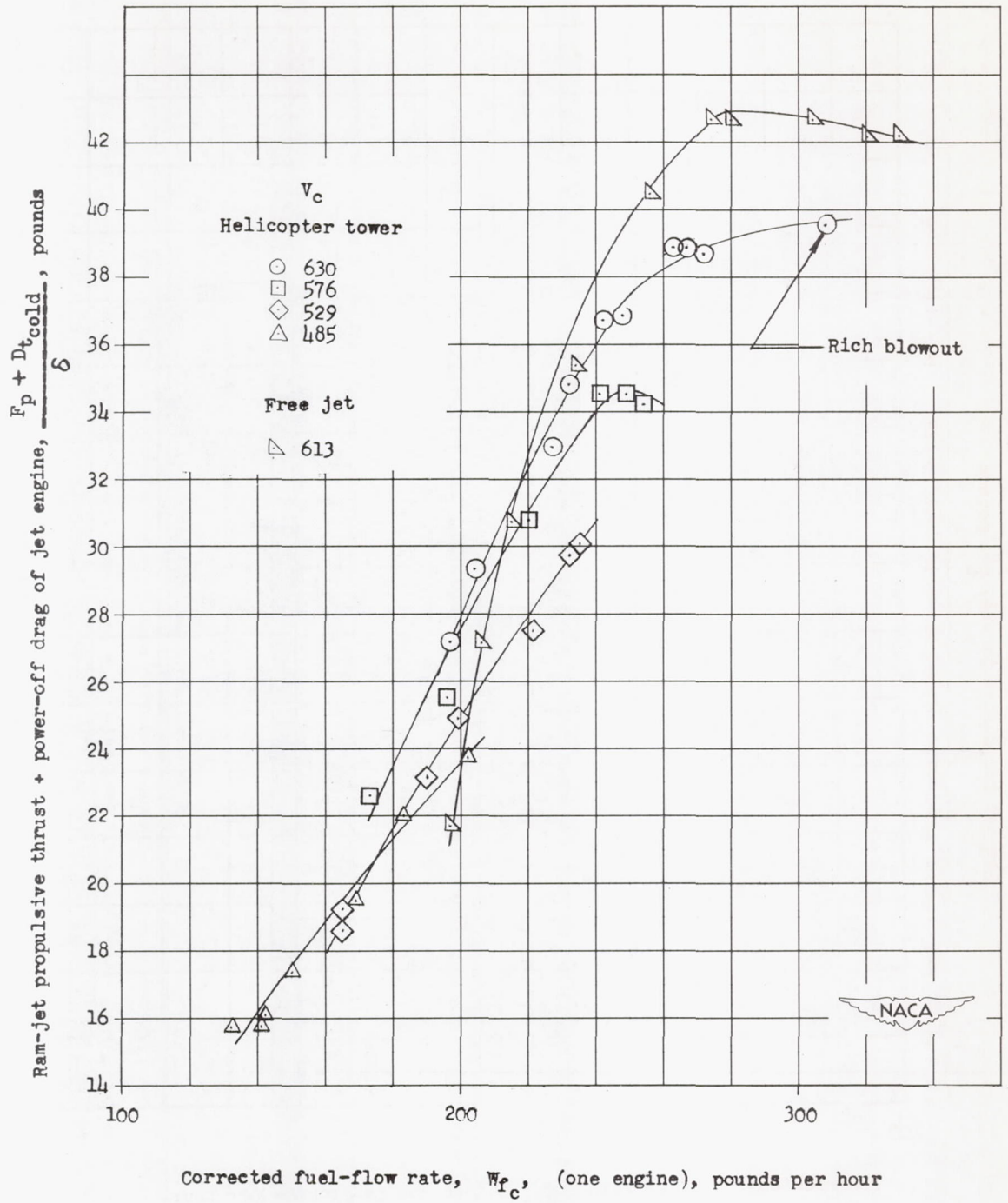

Figure 8.- Corrected ram-jet propulsive thrust plus power-off drag against corrected fuel consumption for one engine. Values for rotor tests are corrected from ambient temperature plus a 50° F rise in tip path plane due to contamination.

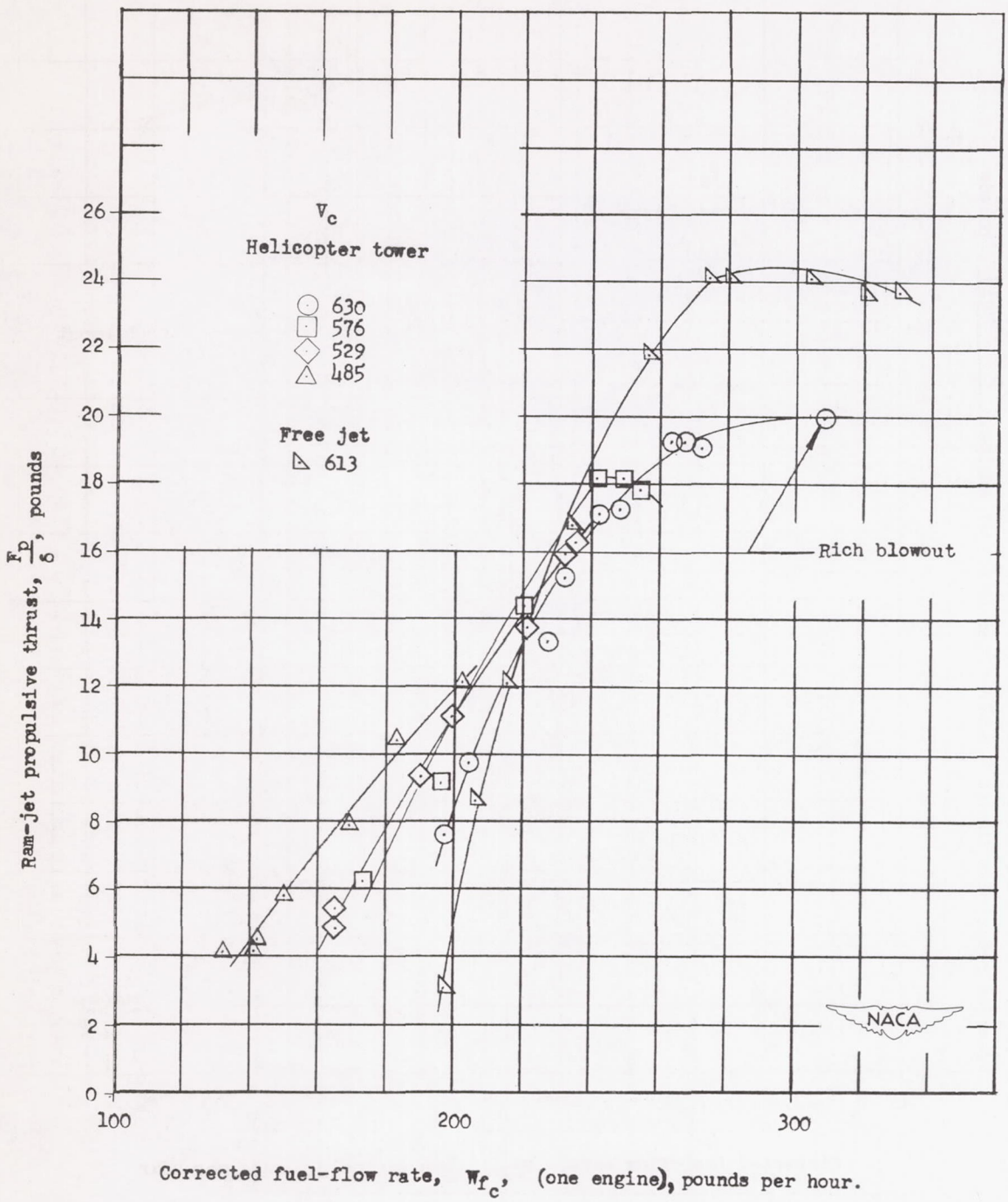

Figure 9.- Corrected ram-jet propulsive thrust against corrected fuel consumption. Values for rotor tests are corrected from ambient temperature plus a 50° F rise in the tip path plane due to contamination.

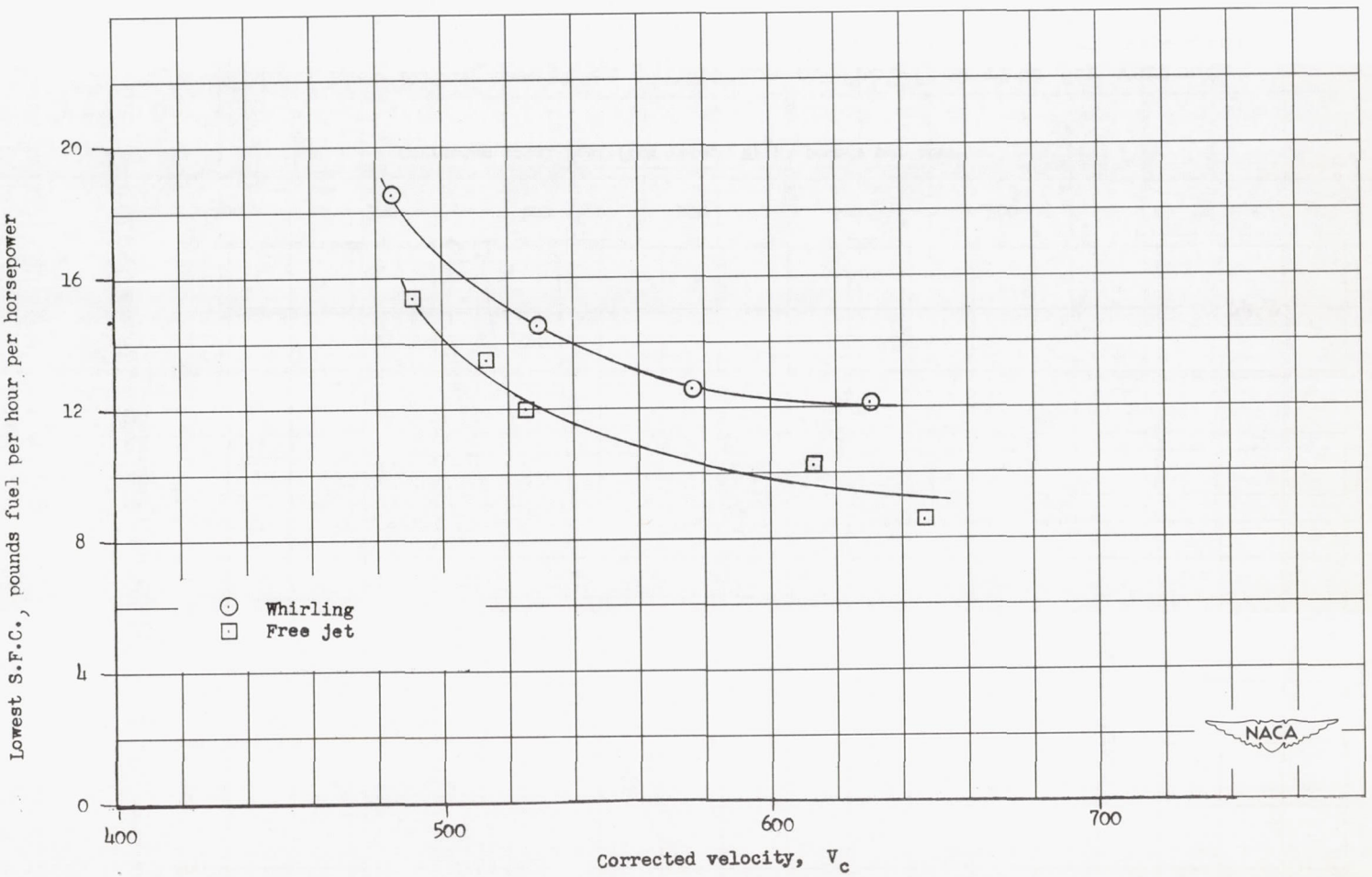

Figure 10.- Comparison of lowest specific fuel consumption for whirling and free-jet thrust-stand test conditions corrected to standard sea-level conditions. V_c represents whirling data corrected from atmospheric plus a temperature rise of 50° F in the tip path plane due to contamination.

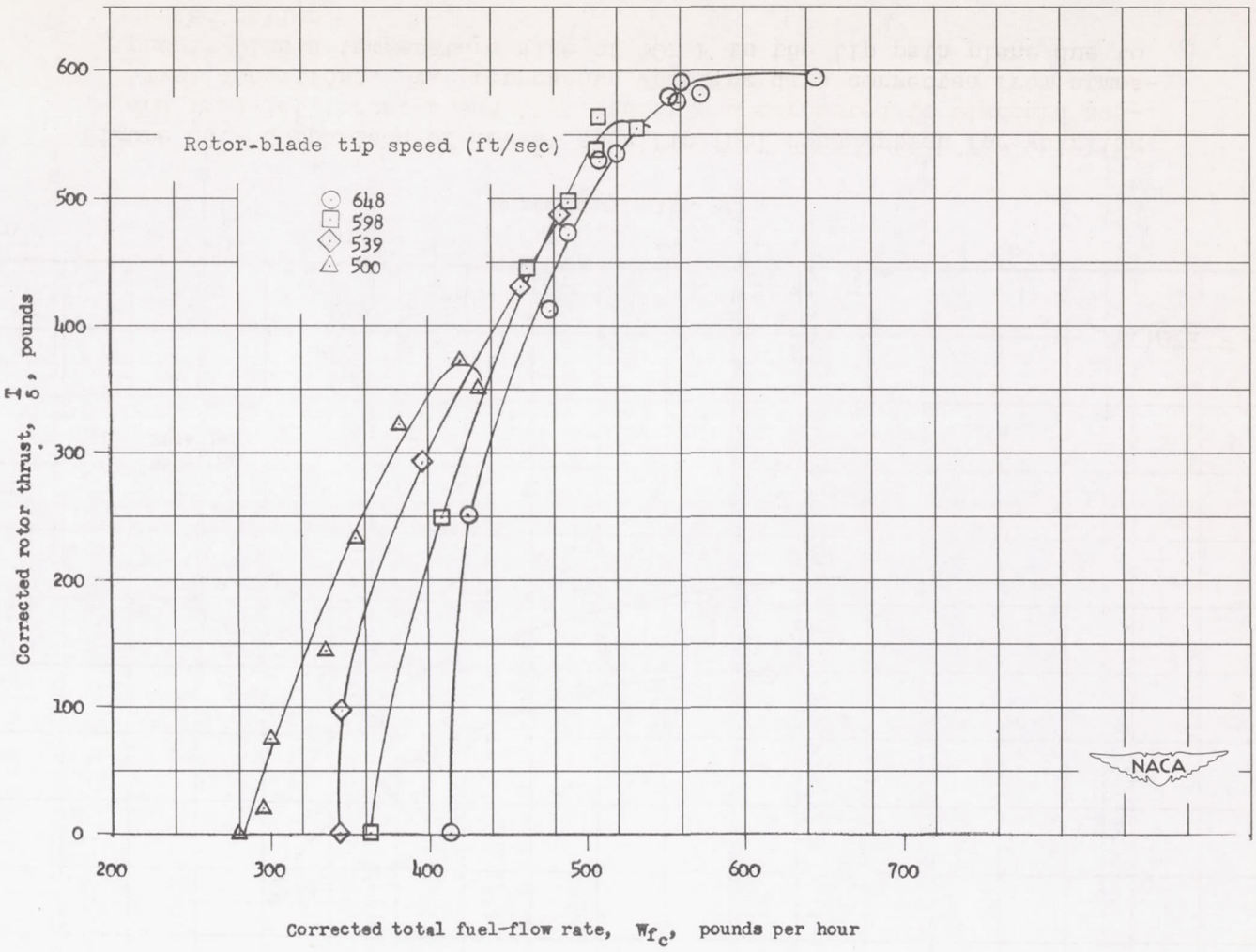

Figure 11.- Rotor thrust as a function of fuel-flow rate for various tip speeds corrected from ambient atmospheric to standard sea-level conditions.

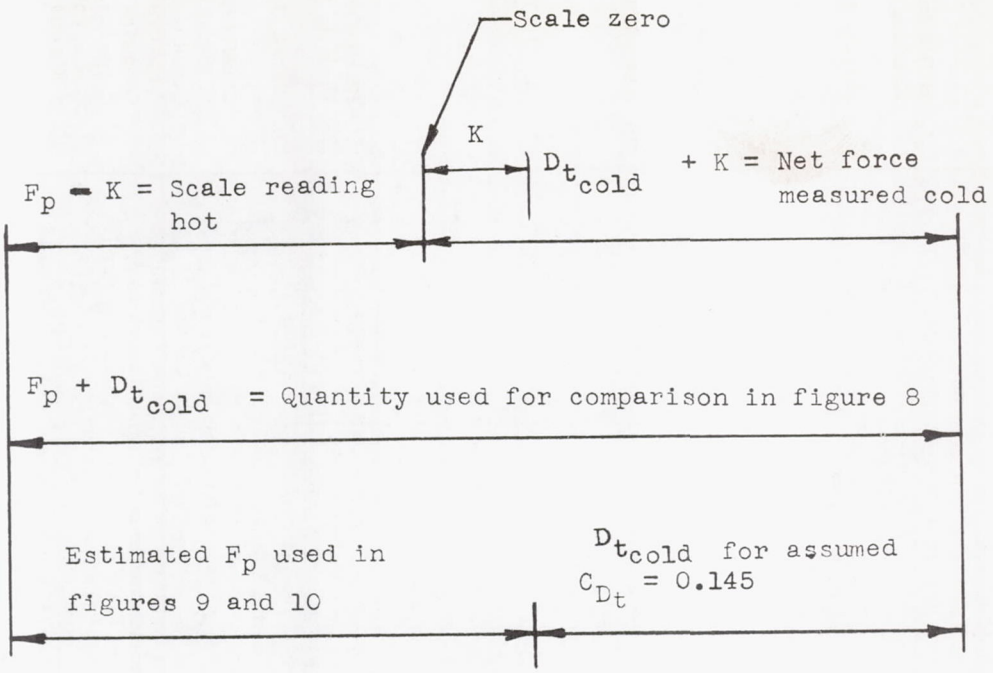

Free-jet thrust-stand tests

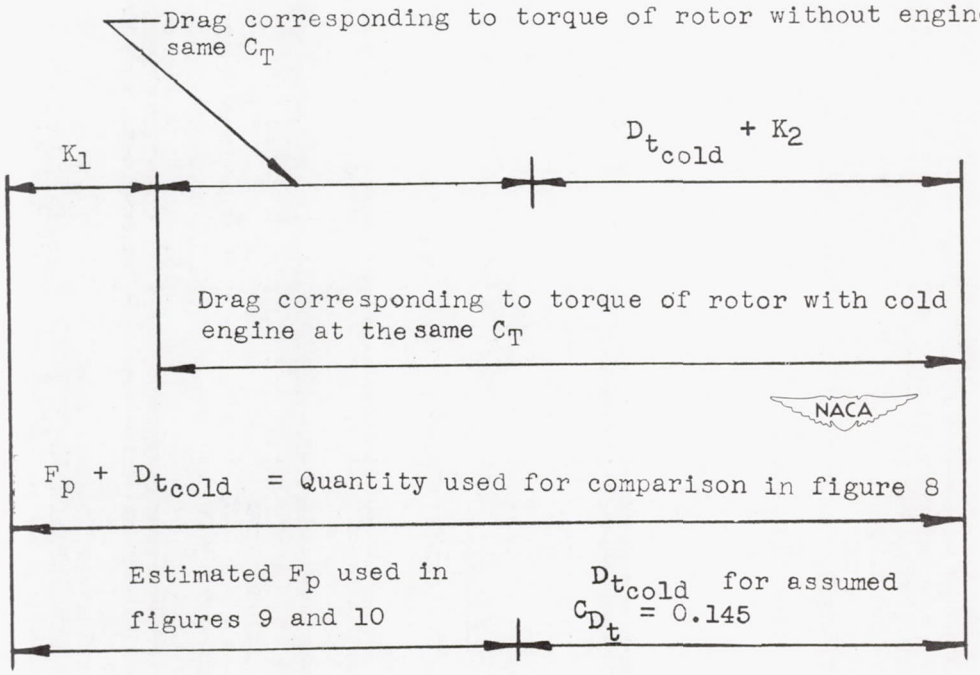

Rotor tests

Figure 12.- Force components used for analysis in the appendix.